DISTRIBUTION OF TOPOGRAPHIC SLOPE AND ROUGHNESS IN MERCURY'S NORTHERN HEMISPHERE. Di Yang[1], Maria T. Zuber[1] James W. Head[2], and Sean C. Solomon[3,4], [1]Department of Earth, Atmospheric and Planetary Sciences, Massachusetts Institute of Technology, Cambridge, MA 02138, USA, [2]Department of Geological Sciences, Brown University, Providence, RI 02912, USA, [3]Lamont-Doherty Earth Observatory, Columbia University, Palisades, NY 10964 USA; [4]Department of Terrestrial Magnetism, Carnegie Institution of Washington, Washington, DC, 20015, USA.

Introduction: The Mercury Laser Altimeter (MLA) [1], an instrument on the MErcury Surface, Space ENvironment, GEochemistry, and Ranging (MESSENGER) spacecraft [2,3], is measuring surface elevations on Mercury with a precision of less than 1 m [4]. MLA topography in combination with high-resolution digital images from the Mercury Dual Imaging System (MDIS) [5] permits quantitative characterization of geological terrains [6, 7], following approaches implemented with measurements by the Mars Orbiter Laser Altimeter (MOLA) [8] and Lunar Orbiter Laser Altimeter (LOLA) [9] to characterize topographic slopes and roughness of geological units on Mars [6, 7] and the Moon [10], respectively.

In this study, we present a roughness map of Mercury's northern hemisphere and compare it to geologic units identified on the basis of surface morphology, reflectance, and color from Mariner 10 MESSENGER images. For low-latitude regions that contain fewer MLA passes we calculated roughness along track, and we correlate roughness with along-track topography. For all terrains studied, we present the scale dependence of roughness and discuss distinctive patterns.

Methodology: *Differential Slope.* To estimate characteristic roughness at the given length scale of interest, the regional topographic trend must be removed. Following the method of differential slope [11], we employ a point counting method rather than define an precise baseline length because of the uneven spatial distribution of MLA data [12].

Roughness. The median absolute value of all differential slopes calculated at a given baseline within an area of interest is taken to be its roughness.

Results: *Northern Hemisphere.* A synoptic visualization of both the general roughness of the surface and the dependence of roughness on baseline length is shown in Fig. 1. Brighter colors denote rougher surfaces. The most striking characteristic in Fig. 1 is the correspondence of roughness boundaries to the boundaries of different geological terrains (Fig. 2). All broad depressions that have been mapped so far are relatively smooth at all baselines, except an area of cratered lowlands (Fig. 2). All highlands are heavily cratered and rougher at all baselines.

Northern Smooth Plains. The lowland region surrounding the north pole, termed the northern smooth plains (Fig. 2) and interpreted to be volcanic flows that flooded and smoothed the underlying heavily cratered terrain [13], is smoother (typical roughness values: red 0.36°, green 0.22°, blue 0.17°) than surrounding terrains (typical values: red 0.9°, green 3.1°, blue 2.1°). A notable topographic feature within the northern smooth plains is the northern rise (Fig. 2) [4]. The roughness map shows no resolvable differences between the northern rise and the surrounding plains. The surface morphology of the rise as seen from images is also similar to that of the surrounding smooth plains [14].

Caloris Basin. Owing to the latitude of the basin, cross-track spacing of MLA data is larger than for the polar region. Consequently, roughness can be biased since longitudinal variations need not be accurately reflected by along-track slopes. Despite non-optimal sampling, the roughness map still demonstrates the distinctive geologic characteristics of the area (Fig. 1). The roughness boundary of Caloris is nearly coincident with the geological boundary (Fig. 2) of its interior plains [15, 17]. The relatively smooth areas between the center of the basin and the Caloris Montes Formation are covered by interior plains materials that are interpreted to be volcanic in origin [15, 16]. A single profile analysis is shown in Fig. 3, which samples the midline of Caloris basin and crosses several major formations, including the Caloris Montes, concentrically arrayed wrinkle ridges, and the central Pantheon Fossae and associated Apollodorus crater [18, 19]. The long-baseline roughness (Fig. 3) is sensitive to large-scale variations such as the Caloris Montes and large impact craters, whereas short-baseline roughness is sensitive to persistent variations at higher wave number, such as the graben of Pantheon Fossae [20]. The intermediate-baseline roughness reflects aspects of variations at both large and small spatial scales.

Heavily Cratered Areas. In contrast to the basins and depressions that exhibit relatively smooth surfaces, the more heavily cratered highlands in the northern hemisphere are generally rough (bright) in Fig. 1. The predominant green color in Fig. 1 reflects the rough surface caused by dense cratering. An area of cratered lowlands at high northern latitudes (Fig. 2) is not readi-

ly distinguishable from the surrounding highlands (Fig 1) on the basis of roughness. Intercrater plains consist of moderately to markedly rough surfaces (green and brighter green in color, respectively, in Fig. 1). Large craters with plains materials on their floors are smooth (dark) in the map.

Scale Dependence of Roughness. The scale dependence of roughness of five major units in the northern hemisphere (Fig. 4) can assist in terrain characterization and analysis. These curves cluster into two groups. Each group has similar roughness values, and similar scale-dependent patterns. Two regions of highlands (Fig. 2) are almost identical at all scales in terms of roughness. The cratered lowlands are even rougher than the cratered highlands due primarily to an ancient basin and larger numbers of superposed relatively fresh craters. A hockey-stick-shaped curve is characteristic of heavily cratered surfaces. All smooth plains, in contrast, follow power laws of roughness versus scale.

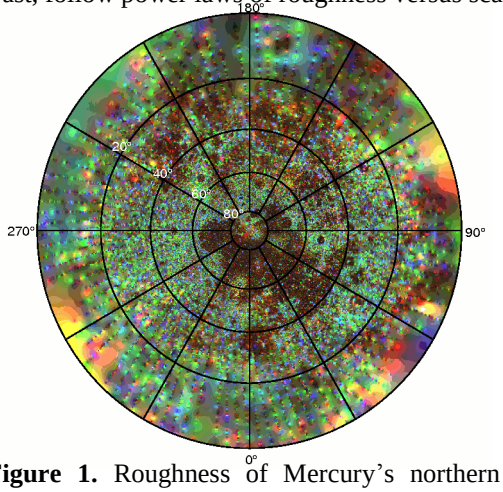

Figure 1. Roughness of Mercury's northern hemisphere (red channel: ~0.8-km baseline; green channel: ~3.2-km baseline; blue channel: ~12.8-km baseline).

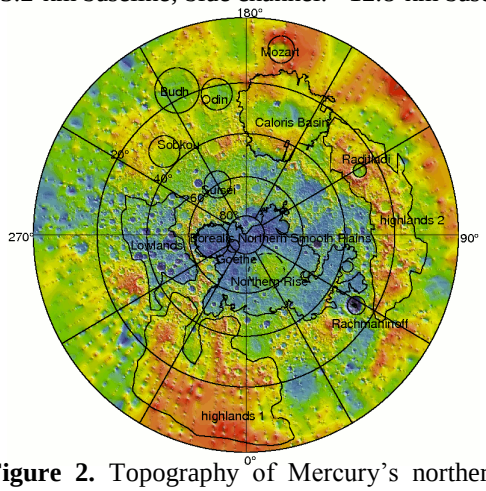

Figure 2. Topography of Mercury's northern hemisphere. Geologic regions discussed in this work are outlined in black.

References: [1] Cavanaugh J. F. et al. (2007), *Space Sci. Rev. 131*, 451-480. [2] Solomon S. C. et al. (2001), *PSS 49*, 1445-1465. [3] Solomon S. C. et al. (2007) *Space Sci. Rev. 131*, 3-39. [4] Zuber M. T. et al. (2012) *Science 336*, 217-220. [5] Hawkins S. E. et al. (2007) *Space Sci. Rev. 131*, 247-338. [6] Aharonson O. et al. (1998) *GRL 25*, 4413-4416. [7] Kreslavsky M. A. and Head J. W. (1999) *JGR 104*, 21911-21921. [8] Zuber M.T. et al. (1992) *JGR 97*, 7781-7797. [9] Smith D. E. et al. (2010) *GRL 37*, doi:10.1029/2010GL043751. [10] Rosenburg M. et al. (2011) *JGR 116*, doi:10.1029/2010JE003716. [11] Kreslavsky M. A. and Head J. W. (2000) *JGR 105*, 26695-26626. [12] Yang D. et al. (2013) *JGR*, in preparation. [13] Head J.W. et al. (2011) *Science, 333*, 1853-1856. [14] Dickson J. L. et al. (2012) *LPS 43*, 2249. [15] Murchie S. L. et al. (2008) *Science 321*, 73-76. [16] Head J. W. et al. (2008) *Science 321*, 69-72. [17] Solomon S. C. et al. (2008) *Science 321*, 59-62. [18] Watters T. R. et al. (2009) *EPSL 285*, 309-319. [19] Basilevsky A. T. et al. (2011) *Solar Sys. Res. 45*, 471-497. [20] Watters T. R. et al. (2005) *Geology 33*, 669-672.

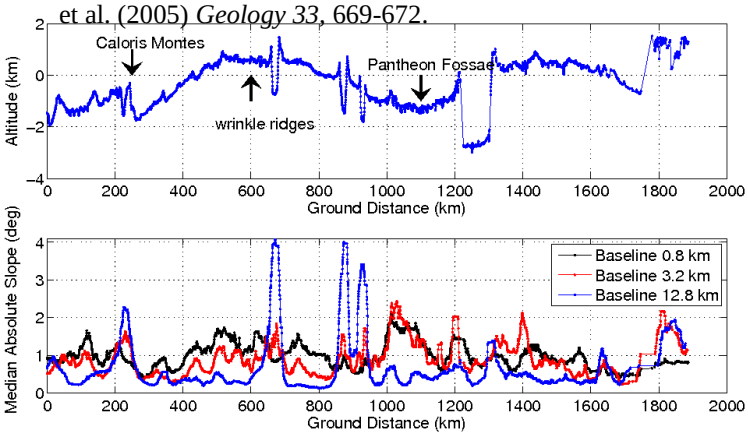

Figure 3. Topographic profile (upper panel) across Caloris basin. Roughness curves (lower panel) at short and intermediate baselines peak at the locations of troughs and ridges. The curve at the longest baseline peaks at the locations of craters.

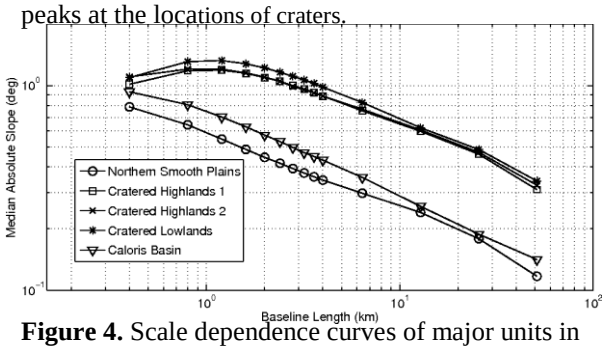

Figure 4. Scale dependence curves of major units in Mercury's northern hemisphere. The roughness of smooth units decays as a power law with increasing baseline lengths, while the scale dependence curves of heavily cratered units are of hockey stick shape.